Spin Decay of Liquid-Filled Projectiles

C. W. Kitchens Jr.,* N. Gerber,† and R. Sedney‡
Ballistic Research Laboratory, Aberdeen Proving Ground, Md.

An accurate method is described for predicting the spin decay of spin-stabilized liquid-filled projectiles throughout their flight. The method is based on a physical model for the spin-up of the liquid payload. Results are compared to spin-decay measurements obtained from test firings of 155-mm liquid-filled projectiles equipped with solar aspect sensors. For most rounds a smooth spin record is obtained and the predicted spin agrees with the measurements to within 1%. A few rounds with large first maximum yaw have a different type of spin record exhibiting an almost discontinuous spin decay rate. An explanation for these cases is put forth which depends on a conjectured instability of the flow. A moderately successful criterion for predicting these cases is developed.

Introduction

THE spin of all projectiles decreases along the flight path because of skin friction on the exterior surface of the casing. Some shells, however, contain liquids; and the spin of a liquid-filled shell decreases more rapidly than that of one with a solid payload. This happens because angular momentum is transferred from the projectile casing to the liquid payload while the liquid is being spun up. Shell containing chemical payloads and smoke/incendiary agents are typical of liquid-filled projectiles of interest to the Army.

A study of the liquid spin-up and projectile spin-decay processes are important for several reasons. First, the frequencies of free oscillation of the liquid change during spin-up and are needed to analyze the flight stability of a liquid-filled shell. Second, spin decay can decrease the gyroscopic stability factor of a liquid-filled shell to an unacceptable level. Third, the projectile spin-decay process may possibly lead to fluid-dynamic instabilities in the liquid payload which could affect the shell motion.

The basis of the present work is a theory developed by Wedemeyer[1] which describes spin-up from rest of a liquid in a fully filled cylindrical cavity. This theory accounts for a secondary flow, formed in the cavity as a result of the endwall boundary layers, which controls the spin-up process. Wedemeyer developed an equation for the azimuthal velocity during spin-up which he solved in closed form by neglecting viscous diffusion terms. He used this solution to derive approximate expressions for the rate of change of angular momentum of the liquid and to calculate spin decay of liquid-filled projectiles.

We also calculate spin decay with Wedemeyer's equation, but our analysis differs from Wedemeyer's in several respects. First, we retain the viscous diffusion terms he neglected. Second, our analysis includes a treatment of the nonimpulsive spin-up within the gun. The accuracy of this techique is evaluated by comparing its results with numerical solutions of the Navier-Stokes equations. Third, we include the aerodynamic spin-damping effect.

Spin-decay predictions obtained here are compared with measurements taken in test firings of 155-mm projectiles using a solar aspect sensor and telemetry technique.[2] The predicted spin decay agrees to within 1% with the measurements except for some firings where the projectiles were launched with large yaw. In these cases the spin history is characterized by a rapid initial spin decay, which is linear for 1 to 2 s, followed by a sharp change to a smaller rate or decay. We conjecture that a nonlinear instability during spin-up creates toroidal vortices which account for the rapid initial spin decay. A flow model and a torque estimate are used to predict a spin-decay history which is consistent with that measured in experimental firings.

Projectile Spin-Decay Equations

Consider a projectile with a liquid-filled cylindrical cavity. Translational motion of the projectile in the gun brings the projectile casing up to the launch spin rate, p_0, because of the barrel rifling. Spin-up of the liquid begins in-bore and continues after the projectile exits the gun tube. In free flight the spin rate, p, of the projectile begins to decrease from its launch value because of two moments produced by shear forces: 1) spin-decelerating moment due to air shear, M; and 2) liquid-shear torque, T, which causes angular momentum transfer between the casing and the liquid. In all equations p is expressed in units of rad/s, but in the figures units of rev/s are used to correspond to the experimental data. The projectile spin rate is determined from the equation of motion,

$$I_z \mathrm{d}p/\mathrm{d}t = T + M \tag{1}$$

where

$$T = -\mathrm{d}L/\mathrm{d}t \qquad M = pf(t) \tag{2}$$

and

$$f(t) = \rho_a \bar{V} \bar{S} l^2 C_{l_p}/2 \tag{3}$$

is a known function of time depending on the projectile shape and trajectory. The quantity I_z is the axial moment of inertia of the empty projectile, L is the liquid-axial-angular momentum, $\bar{V}$ is the projectile speed, $\bar{S}$ is the maximum-projectile cross-sectional area, l is the projectile diameter, ρ_a is the air density, and C_{l_p} is the projectile roll-damping coefficient. Since M is negative over the whole trajectory, it causes p to decrease. T, on the other hand, is negative at launch and in the early portion of the trajectory, but positive late in the flight. The liquid spin-up process, with $\mathrm{d}L/\mathrm{d}t > 0$, takes place during the in-bore and early free-flight phases.

Presented as Paper 77-1158 at the AIAA 4th Atmospheric Flight Mechanics Conference, Hollywood, Fla., Aug. 8-10, 1977; submitted Feb. 8, 1978; revision received June 12, 1978.

Index categories: Hydrodynamics; LV/M Testing, Flight and Ground; Viscous Nonboundary-Layer Flows.

*Aerospace Engineer, Launch and Flight Division. Member AIAA.
†Research Aerospace Engineer, Launch and Flight Division. Member AIAA.
‡Chief, Fluid Dynamics Research Group. Associate Fellow AIAA.

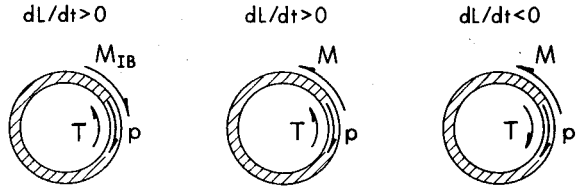

Fig. 1 Moments acting on a spinning liquid-filled projectile – a free-body diagram of casing during launch and free flight.

The moments acting on the casing during these phases are shown in Figs. 1a and b. While the casing spin rate decreases, liquid spin-up proceeds, approaching solid-body rotation; the latter is never achieved because the aerodynamic moment continues to decrease the projectile spin rate. The liquid will eventually be "overspun" relative to the instantaneous projectile spin rate; that is, the local angular velocity, $\bar{\omega}=\bar{v}/r$, where $\bar{v}$ is the azimuthal velocity and r is the radial coordinate, will be greater than p. Late in the flight the liquid moment reverses direction (Fig. 1c); i.e., $dL/dt<0$, thus opposing further spin decay of the projectile.

We need to know M and T as functions of p and t in Eq. (1). The first is obtained from flight measurements using a projectile with a solid payload; T is determined by solving the equations of motion for the liquid. The boundary conditions for these equations involve p, which is the quantity we wish to determine. Thus an iteration process is indicated. If the fluid motion is known, T can be found from Eq. (2) using the definition

$$L(t)\equiv\rho\int\int\int r^2\bar{v}(r,z,t)\,d\theta\,dr\,dz \tag{4}$$

where the integral is taken over the cavity volume; r, θ, z are nonrotating cylindrical coordinates with z along the axis of the projectile, and ρ is the liquid density.

In our analysis we neglect the projectile yawing motion and assume that the spin-up flow is axisymmetric. Wedemeyer's spin-up theory[1,3] is used to determine $\bar{v}$.

Calculation of Liquid Angular Momentum

The Wedemeyer Spin-Up Model

Wedemeyer[1] considered the problem of a circular cylinder filled with liquid which is initially at rest. At $t=0$ it is given an impulsive spin about its longitudinal axis, which is maintained thereafter. He determined the resulting unsteady flow. The flow region is divided into two parts: 1) the thin Ekman boundary layers on the cylinder endwalls; and 2) the remainder of the flow, called the core flow. It is found that the spin-up process is dominated by the Ekman layers. These layers induce centrifugal pumping which causes secondary flow in the core. This flow enters the Ekman layers at r $(0<r\leq r^*)$, is spun up, and then ejected back into the core at $r>r^*$, where r^* is the radial position of a shear layer which propagates inward from the sidewall. This spinning fluid is then convected into the interior of the cylinder. This mechanism of imparting rotation to the fluid is much more efficient than viscous diffusion alone.

Wedemeyer developed an approximate equation for the core flow through an order of magnitude analysis of the axisymmetric Navier-Stokes equations. In the core the tangential velocity component $\bar{v}(r,z,t)$ becomes $v(r,t)$, and v is determined as the solution to the core-flow equation:

$$\frac{\partial v}{\partial t}+u\left(\frac{\partial v}{\partial r}+\frac{v}{r}\right)=\nu\left[\frac{\partial^2 v}{\partial r^2}+\partial\frac{(v/r)}{\partial r}\right] \tag{5}$$

where u is the radial velocity component and ν is the liquid kinematic viscosity. His analysis shows that u and the axial velocity w, the secondary flow referred to above, are small compared to v, but not negligible, and that u and v are independent of z. Conservation of mass relates u to the outward radial mass flow in the Ekman layers. An assumption is then made for the relation between the Ekman layer mass flow and v by interpolating between the known results for $t\to 0$ and $t\to\infty$.

Wedemeyer obtained two relationships for u depending on whether the endwall boundary layers were expected to be laminar or turbulent:

$$u=-0.443(a/c)Re^{-1/2}(rp-v) \tag{6}$$

for $Re<3\times10^5$ and

$$u=-0.035(a/c)Re^{-1/5}(rp-v)^{8/5}/(ap)^{3/5} \tag{7}$$

for $Re>3\times10^5$; where c is the cavity half-height, a is the cavity radius, and the Reynolds number is

$$Re=pa^2/\nu \tag{8}$$

In his formulation of the spin-up problem he assumes p is constant, but in his application to spin decay p is a function of time. We shall also allow p to be a function of time.

The initial and boundary conditions for Eq. (5) are

$$v(r,t)=0 \quad \text{for} \quad t<0$$

$$v(0,t)=0 \quad \text{and} \quad v(a,t)=ap \quad \text{for } t\geq 0 \tag{9}$$

During projectile in-bore travel $p(t)$ is specified; it is obtained from an interior ballistics trajectory. In free flight $p(t)$ cannot be independently specified; it must be calculated from Eq. (1). The total angular momentum of the liquid within the cylinder can be expressed using Eq. (4) with $\bar{v}$ equal to v:

$$L=4\pi c\rho\int_0^a r^2 v\,dr \tag{10}$$

Computation Procedures

In calculating the spin decay of liquid-filled shell, we used two methods, designated I and II.

In method I, calculations are performed by simultaneously solving Eqs. (1), (5), and (10), using Eqs. (2) and (3). Equation (5) is solved by a second-order accurate finite-difference technique.[3] We assume that all variables are known at time t_n, and we wish to determine p and L at time t_{n+1}. We approximate Eq. (1) by a second-order accurate finite-difference expression and solve for p_{n+1}, obtaining

$$p_{n+1}=\frac{p_n[I_z+\Delta t f(t_n)/2]-L_{n+1}+L_n}{[I_z-\Delta t f(t_{n+1})/2]} \tag{11}$$

which relates the spin and angular momentum at t_{n+1} to $f(t_n)$, $f(t_{n+1})$, p_n, L_n, Δt, and I_z.

The fluid angular momentum L_{n+1} must be calculated from Eqs. (5) and (10) using the sidewall boundary condition $v(a,t_{n+1})=ap(t_{n+1})$. These equations give us a second relationship between p_{n+1} and L_{n+1} which is very complicated. This is combined with Eq. (11) to provide two equations for p_{n+1} and L_{n+1} which are solved numerically. We adopt an iteration procedure on L_{n+1} to retain second-order accuracy. The first iterate for L_{n+1}, L^1_{n+1}, is obtained using values at previous times and solving Eq. (11) for p_{n+1}. Equation (5) is then solved using p_{n+1} as a boundary condition to yield $v(r,t_{n+1})$. The angular momentum L^2_{n+1} is calculated and compared with the guessed value L^1_{n+1}. If they differ by more than a set tolerance, the calculation is repeated using L^2_{n+1} as the guess in Eq. (11). This iteration process is repeated until the desired tolerance is achieved. Convergence was achieved in one to three iterations. This procedure can be

used to treat either laminar or turbulent endwall boundary layers through the specification of Eqs. (6) or (7) for u in Eq. (5).

Method II is a simpler procedure, based on an ordinary differential equation for L which is solved simultaneously with Eq. (1). There are separate equations in the laminar and turbulent cases [Eqs. (42) and (53), respectively, in Ref. 1]. These equations were derived by Wedemeyer assuming that Eq. (5) is valid for nonconstant spin rate. Method II has the disadvantage that the approximations involved in evaluating the shear stress at the sidewall (and the velocity profile in the turbulent case) are not accurate when $dL/dt<0$. More details on spin-decay computations are found in Ref. 4.

In-Bore Spin-Up Effects

The first step in calculating projectile spin decay is to determine the angular momentum acquired by the liquid during in-bore spin-up. This prescribes the initial conditions for the subsequent spin-decay calculation. As a reference value for angular momentum we use $L_0=\pi\rho ca^4p_0$, the value for the fluid in solid-body rotation, with $v=p_0r$. The angular momentum achieved at the muzzle exit, relative to L_0, is determined by the launch Reynolds number,

$$Re_0=p_0a^2/\nu \tag{12}$$

In-bore, the shell is given a large angular acceleration. We assume that Wedemeyer's equation based on impulsive spin-up, Eq. (5), can be used in cases where the spin acceleration is very large. (For cases treated here, the spin acceleration is more than 4,800 rev/s^2. A typical 155-mm shell accelerates to a spin rate $p_0=92$ rev/s, corresponding to a muzzle velocity $V_0=285$ m/s, in 19 ms after firing.) The in-bore shell motion, predicted using an interior ballistics trajectory computer program, is used together with the gun twist to determine the casing spin-rate boundary condition. In method I the instantaneous p at each t is used in Eq. (5), the expressions for u, and the boundary conditions.

Figure 2 shows predictions for the in-bore angular momentum history for two 155-mm shell; t^* is time measured from beginning of in-bore motion. Round 1 contains a highly viscous oil ($\nu=5\times10^{-4}$ m^2/s); with $Re_0=3320$, Eq. (6) is used. This calculation predicts that the liquid angular momentum is 18.6% of L_0 at shell exit. Round 2 contains water ($\nu=1\times10^{-6}$ m^2/s) and so $Re_0=1.7\times10^6$; therefore, the turbulent endwall boundary-layer assumption, Eq. (7), is used. The water payload spins up much more slowly than the oil, acquiring only 2.6% of L_0 at the muzzle exit.

As a check on the accuracy of these results a finite-difference procedure was used to solve the Navier-Stokes equations.[5] The flow is assumed axisymmetric; it is calculated without separating the problem into boundary layer and core regions. Results from the Navier-Stokes solution for round 1 are shown by the dashed curve in Fig. 2. This calculation predicts an angular momentum level that is 2.5% larger at the muzzle exit than that predicted by method I. The discrepancy between these two calculations remains almost constant after about 6 ms. A Navier-Stokes calculation has not been made for round 2 because of the expected turbulent flow in the endwall boundary layer. On the basis of the comparisons for round 1, we feel justified in using method I, based on Wedemeyer's spin-up model, for predicting the in-bore angular momentum history of the liquid.

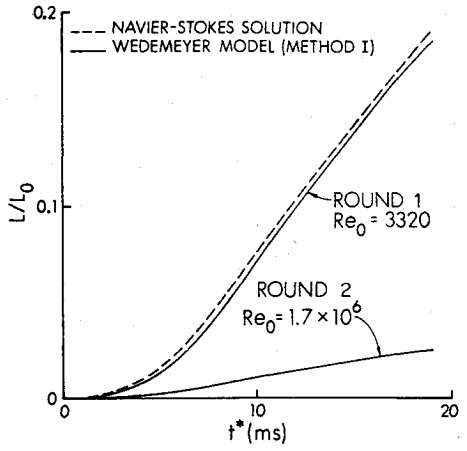

Fig. 2 Normalized in-bore liquid-angular-momentum history for two 155-mm liquid-filled projectiles with different launch Reynolds numbers.

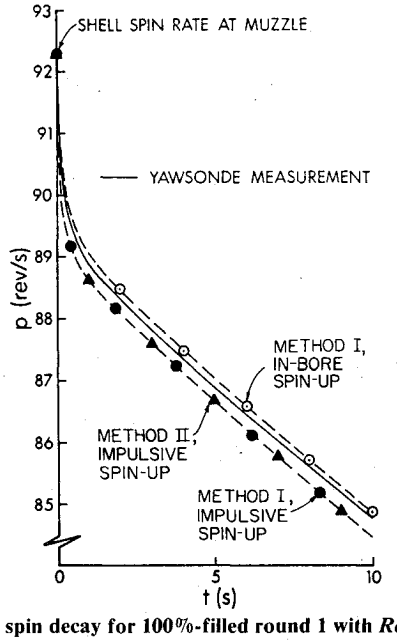

Fig. 3 Shell spin decay for 100%-filled round 1 with $Re_0=3320$ and laminar Ekman layer.

Comparison with Measured Spin Decay

Spin-decay predictions have been made for 155-mm liquid-filled shell and compared with measurements obtained using a solar aspect sensor and telemetry technique.[2] The motion of the projectile is determined by the use of photovoltaic cells which sense the orientation of the shell relative to the sun. The measuring system, called a yawsonde, is carried on-board the projectile and data are transmitted to a ground station through an FM/FM telemetry link. Data are first received shortly after the shell exits from the gun tube. The data reduction procedure yields both the yawing motion of the projectile and the spin history over the whole trajectory.

In order to compare flight data with the present theory, rounds with a modified payload cavity were chosen; namely, a single cylindrical cavity having a height of $2c=0.474$ m and a diameter of $2a=0.107$ m. Fill ratios of both 90 and 100% were used in the firing program. For all calculations discussed here the spin damping coefficient was described by

$$C_{l_p}=0.00860\bar{M}-0.0200 \quad \text{for} \quad 0.53\le\bar{M}\le0.84 \tag{13}$$

where $\bar{M}$ is the instantaneous Mach number. Equation (13) was determined from firings with a solid payload. The air density and temperature needed to define the spin damping function in Eq. (3) were determined from meteorological data, and the projectile speed was deduced from radar measurements. For the cases to be discussed, the $f(t)$ of Eq. (3) for rounds 1-4 is presented in Fig. 4 of Ref. 4 (labeled "Round 7675"), and for rounds 5 and 6 is given by

$$f(t)=(1.25t-13.5)\times10^{-4}\text{kg-m}^2/\text{s} \quad \text{for} \quad 0\le t\le3\text{s}$$

A nominal value of $I_z=0.163$ kg-m^2 applies to all rounds.

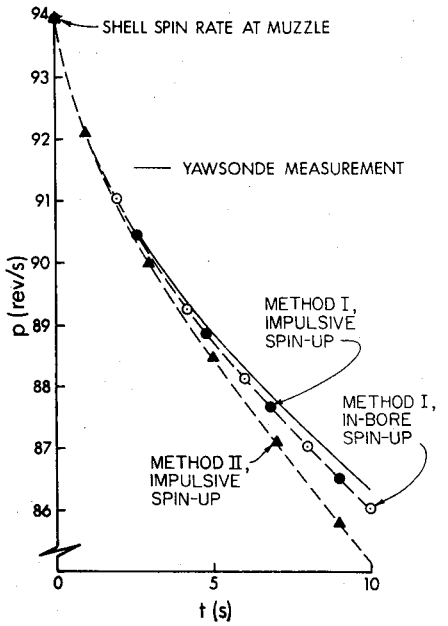

Fig. 4 Shell spin decay for 100%-filled round 2 with $Re_0 = 1.7 \times 110^6$ and turbulent Ekman layer.

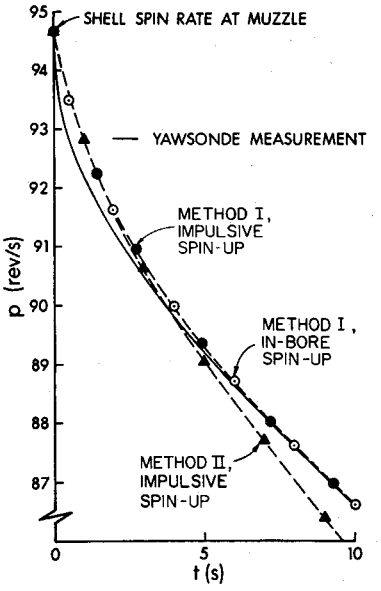

Fig. 5 Shell spin decay for 90%-filled round 4 with $Re_0 = 1.7 \times 10^6$ and turbulent Ekman layer.

Filled Shell

The predicted spin decay for round 1 is compared with the yawsonde measurement in Fig. 3. The time when the projectile exits the gun tube is $t = 0$. The total time of flight was 28 s. The spin-up process was completed within 10 s. The spin-decay history deduced from the yawsonde measurement is shown by the solid curve. The spin at the muzzle was calculated from the gun tube twist and independently measured muzzle velocity. Data acquisition began 0.1 s after launch, and the measured data curve was faired back smoothly to the spin at the muzzle.

In the theoretical results shown in Fig. 3 (note the broken ordinate scale) the endwall boundary layers were assumed to be laminar. Results from method I, assuming an impulsive start, are shown by the filled circles; those from method II are shown by the filled triangles. The calculated spin-decay rates are almost identical and are larger than the observed decay rate. At $t = 10$ s the difference in p is 0.4%. With in-bore effects included, results from method I agree better with the measurements, as shown by the open circles in Fig. 3. The in-bore spin-up process described previously was used for the 19 ms prior to $t = 0$. Spin-up was completed at $t = 1.4$ s; for $t > 1.4$ s the shell is in the late free-flight phase, shown in Fig. 1c, wherein the direction of the liquid moment reverses. At this time the predicted p, including in-bore effects, was 0.13% larger than the measured value.

When the launch Reynolds number is greater than 3×10^5 the endwall boundary layers are expected to be at least partially turbulent. The measured spin decay for round 2, with a water payload, is compared with predictions assuming a turbulent Ekman layer in Fig. 4. Methods I and II both predict a more rapid spin decay than is observed. Method I gives better agreement with the measurement. At this large Re_0, in-bore effects are not significant and both calculations with Method I give essentially the same result. Spin-up takes longer to complete in this case because of the much higher Reynolds number. The predicted time of the reversal of the liquid moment is 24.5 s. At this time the predicted spin rate is 0.79% lower than the measurement, as extrapolated from the available yawsonde data which end at 23.9 s.

Partially Filled Shell

A spin-up model for a partially filled cylinder does not exist. Since most liquid-filled shell are partially filled, it is useful to learn if the methods developed for the filled cylinder can be applied with any confidence to these cases. We might expect this if the fill ratio, β, is not much less than, say, 0.90-0.95.

The Wedemeyer spin-up theory[1] has been applied to a partially filled shell, treating it as though it were fully filled. The spin history for two 155-mm shell (again having a single cylindrical cavity) with $\beta = 0.90$ are compared with predictions. The spin history for round 3 (not shown here), with $\beta = 0.90$ and $Re_0 = 3421$, is almost identical to that observed for the filled case shown in Fig. 3. Methods I and II both give reasonable agreement with the measured spin decay. Method I, including in-bore effects, is slightly more accurate; at 10 s it predicts a spin rate that is 0.18% larger than the yawsonde measurement, whereas method II predicts a value that is 0.29% smaller.

Comparisons for a higher Reynolds number are shown in Fig. 5 for round 4 which is 90%-filled with water. The endwall boundary layers are assumed turbulent. The spin history is qualitatively different than that observed for the 100%-filled case in Fig. 4. The most noticeable difference occurs in the first few seconds of the flight; the 90%-filled case loses spin faster than the 100%-filled case. In the first half-second of flight the 90%-filled case losses 2.0% of its muzzle spin rate, whereas the 100%-filled case only loses 1.2%. The longitudinal shifting of the liquid in the partially filled case in-bore and early in the flight possibly enhances mixing the rotating fluid near the sidewall with the fluid in the interior. This motion may account for the more rapid spin decay observed with the partially filled case.

Figure 5 shows that the theory predicts a more gradual spin decay in the first few seconds of the flight than is observed for the $\beta = 0.90$ round. Method I gives a more accurate prediction than method II. Both calculations with method I are almost identical because in-bore effects are small. At $t = 10$ s, method II predicts a spin rate which is in error by approximately 1%, while method I essentially matches the experimental measurement.

Spin-Up Time

The instantaneous state of fluid rotation is determined from the numerical solution of Eq. (5). Solid-body rotation is never achieved because p is constantly changing, but it is more closely approached for small Re_0 because diffusion effects are greater. Figure 6 shows normalized liquid azimuthal velocity profiles predicted with method I, including in-bore effects, at three instants in the flight of round 2. The velocity at the

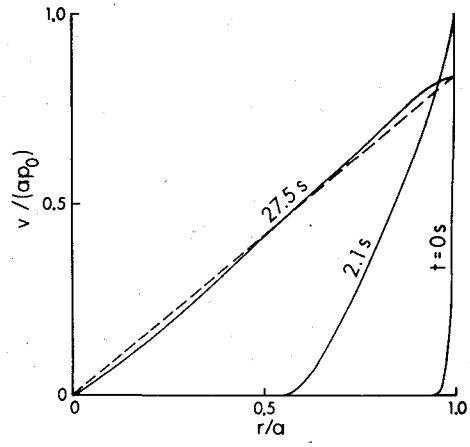

Fig. 6 Azimuthal velocity profiles for round 2 with $Re_0 = 1.7 \times 10^6$ and turbulent Ekman layer.

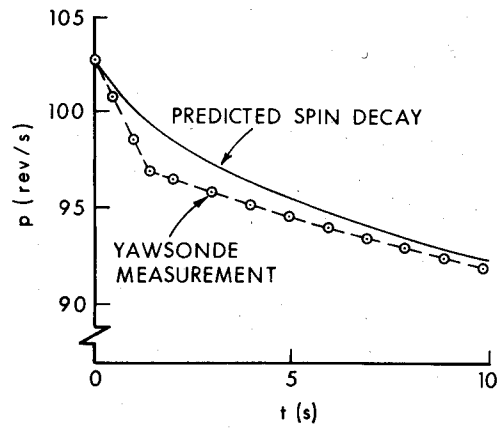

Fig. 7 Comparison of measured and predicted spin decay for 87%-filled round 5 with $Re_0 = 8.7 \times 10^5$, $\alpha_0 = 8.8$ deg, and turbulent Ekman layer.

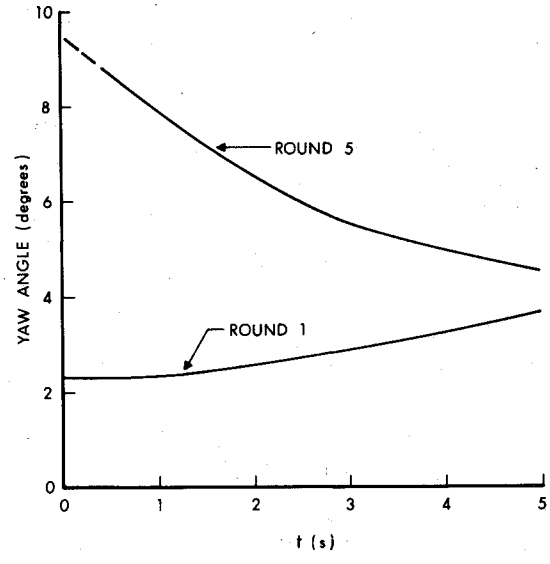

Fig. 8 Comparison of yaw angle histories for rounds 1 and 5.

sidewall, $r/a = 1.0$, decreases with time. A typical velocity profile for solid-body rotation is shown for $t = 27.5$ s by the dashed straight line $v = rp$; however, at $t = 27.5$ s, $v < rp$ for $0 < r/a < 0.57$ and $v > rp$ for $0.57 \leq r/a < 1$. The fluid in the latter range of r is "overspun" relative to the projectile at this time; i.e., the local fluid angular velocity is greater than p. Shortly after the liquid near the sidewall becomes overspun T reverses direction, opposing M (Fig. 1c).

A unique definition of spin-up time is not possible because of the asymptotic approach to solid-body rotation. Depending on the application, different measures of spin-up time are appropriate. A comparable situation exists in defining the thickness of a boundary layer. We adopt a definition based on the calculations of method I. The spin-up time, t_s, is defined to be the time, measured from $t = 0$, at which the fluid angular momentum reaches 99% of the rigid-body angular momentum, L_r, where the latter is based on the instantaneous shell spin rate p. We find that $t_s = 0.9$ s for round 1 and $t_s = 19.0$ s for round 2. The large difference in values of t_s results from the factor of 10^3 difference in Reynolds number.

These results do not agree with those in Ref. 2, in which the instantaneous liquid angular momentum is calculated by fitting measured yawsonde spin rate data and numerically integrating the projectile roll equation. For a typical 155-mm projectile with $Re_0 = 1.7 \times 10^6$, it is concluded that only 85% of L_r is achieved in the 30-s time of flight. The present calculations predict that 85% of L_r is achieved in approximately 7.0 s for round 2 with $Re_0 = 1.7 \times 10^6$. The large difference between these results appears to be caused by the inaccurate value for C_{l_p} used in Ref. 2 and the neglect of in-bore effects. More recent work by the authors of Ref. 2 shows better agreement with our results.

Spin Decay with a Corner

The spin-decay records presented thus far are all smooth curves; we designate these "type S." The rounds in Figs. 3, 4, and 5 were all launched with small yaw using a 155-mm howitzer with a standard muzzle brake; α_0, a measure of the first maximum yaw angle, was less than 4 deg. α_0 was obtained either by extrapolating the yawsonde record back to $t = 0$, or by taking it to be the first observed yaw angle. These two measures differed at most by 10%. Larger yaw levels were produced using a nonstandard muzzle device fabricated by cutting the standard muzzle brake longitudinally in half and welding on side plates. This device created an asymmetric pressure distribution at the gun muzzle which amplified the shell yaw at launch. When this device was employed, $\alpha_0 \geq 4$ deg was obtained, and a different type of spin record, shown in Fig. 7, was sometimes observed.

This record, for round 5, exhibits a rapid initial spin-decay rate for 1.4 s, followed by a sudden change to a smaller rate of decay. The sharp change in slope, which appears to be almost discontinuous, is referred to as a "corner" in the spin record. Records exhibiting corners are designated "type C." The spin loss observed in the first 1.4 s for round 5 corresponds approximately to the amount of angular momentum transfer needed to bring the liquid up to rigid-body rotation.

It is instructive to compare the spin histories for rounds 1 and 5 with their yaw angle histories, the latter shown in Fig. 8. Both rounds approach a precessional limit cycle of approximately 4 deg, the observed yaw behavior depending on the initial yaw angle. Round 1 has an initial yaw angle of 2.3 deg which increases gradually to 4 deg while round 5 has an initial yaw angle of approximately 9.5 deg which decays to 4 deg after 5 s. The upper curve is extrapolated backward in time from the first observed yaw angle. Only $t < 2$ s is relevant in the consideration of the spin decay with corner. Clearly the yaw history for round 5 is smooth even though the spin history (Fig. 7) is not.

The predicted spin history using method I, including in-bore effects, is compared with the measurement in Fig. 7. At $t = 1.4$ s, the measured spin decay is 70% larger than that calculated. The yawsonde measurement has three distinctive features: 1) the corner, 2) the constant slope from $t = 0$ to the corner, and 3) a value for this slope greater than that predicted by theory. The initial slope is essentially proportional to the liquid torque, T, since M is small. Since there is nothing in the theory that would permit features 1 and 2 and the implied value of T ($\approx I_z dp/dt$), a different mechanism

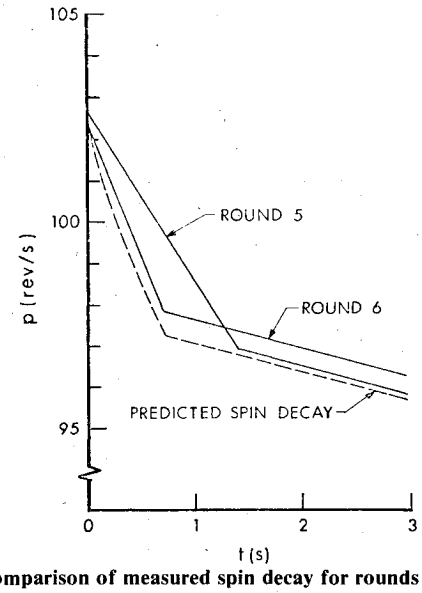

Fig. 9 Comparison of measured spin decay for rounds 5 and 6 with that predicted from the type C flow model.

for spin-up is needed to explain type C records. Laboratory experiments would be required to gain insight into the nature of that mechanism. The available data provide only T; thus our present task is to determine a T that fits the data. Instead of taking a completely empirical approach, we consider possible flow mechanisms and test the resulting values of T against the data.

Flow Mechanisms for Producing a Corner

The firing data show that α_0 and Re_0 are important to the corner question. The parameter α_0 is a measure of the perturbation to the liquid motion, and, in general, Re_0 indicates the stability of this motion. There are not enough data to isolate the remaining parameters and judge their significance. There may be other significant parameters, however. Figure 9 illustrates this possibility for two rounds with essentially the same α_0 and Re_0: round 5 with $\alpha_0 = 8.8$ deg, $Re_0 = 8.68 \times 10^5$, and round 6 with $\alpha_0 = 8.3$ deg, $Re_0 = 8.65 \times 10^5$. For both rounds $\beta = 0.87$. It is most unlikely that the small differences in α_0 and Re_0 can account for the 50% difference in the initial slopes of the two records. Two conclusions seem possible: 1) the firings are reproducible only to within the differences shown for these two rounds; or 2) an unidentified parameter accounts for the differences.

The launch process and/or yaw inducer imparts a perturbation to the projectile; the only observable measure of this is α_0 obtained from the yawsonde data. The question arises, how will this perturbation affect the motion of the liquid? Specifically, will it cause an instability in this motion? Three possible instabilities were considered in detail in Refs. 6 and 7; only an outline is given here.

The first possibility, transition to turbulence in the flow near the sidewall, is plausible. Values of torque from laboratory experiments are available in the literature. These lead to spin-decay rates which are larger than the results from yawsondes by a factor of 2, so this mechanism is rejected. It is possible, however, in the present instance that the axial flow during spin-up and the large (yaw-produced) disturbance in the flow affect the torque to a degree that would render the laboratory data inapplicable.

The second mechanism, centrifugal instability in the perturbation boundary layer at the sidewall, can be rejected because the flow is stable according to an approximate stability analysis.[6,7] For projectiles considered here the value of the Taylor number is ten times smaller than the critical value.

The third possibility is a conjectured nonlinear instability during spin-up. This mechanism could not be ruled out; the

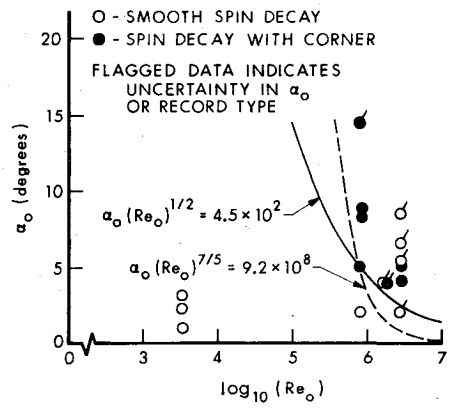

Fig. 10 Comparison of spin record type with $\alpha_0 (Re_0)^{1/2}$ for laminar Ekman layer and $\alpha_0 (Re_0)^{7/5}$ for turbulent Ekman layer.

stability criterion is qualitatively consistent with firing data and the spin-decay prediction is quantitatively consistent with yawsonde results.

Nonlinear Instability During Spin-Up

The spin-up flow is stable with respect to small disturbances, as indicated in Ref. 8. Inviscid centrifugal stability also follows from Rayleigh's criterion, but this criterion cannot be applied when there is axial flow. For the large disturbances considered here, e.g., $\alpha_0 \approx 8$ deg, we conjecture that an instability does occur. Its form is unknown; however, on the basis of several assumptions a torque can be computed which is consistent with the data, despite the tenuous nature of the hypothesis.

For convenience we assume that the instability will result in toroidal vortices adjacent to the cylinder wall, similar to Taylor vortices. The scale of these vortices is determined by the distance between the sidewall and the inviscid front in Wedemeyer's spin-up model.[1] The large scale of these vortices would enhance mixing of spinning with nonspinning fluid and thus decrease the time required for spin-up. The skin friction, with vortices, is greater than that of the Wedemeyer model, producing a higher spin-decay rate. An approximate analysis[6,7] based on this assumption concludes that instability occurs when

$$\alpha (Re_0)^{1/2} > C_3 \qquad \text{(laminar Ekman layer)} \qquad (14)$$

or

$$\alpha (Re_0)^{7/5} > C_4 \qquad \text{(turbulent Ekman layer)} \qquad (15)$$

where C_3 and C_4 are constants. In using these criteria we shall take $\alpha = \alpha_0$.

The firing data were examined to see if the spin record type could be correlated with these instability criteria. Sixteen rounds were available for this test. Except for three rounds, Re_0 is large enough for the expectation of turbulent endwall boundary layers; both criteria are tested, however. From the data we find that critical values of $\alpha_0 (Re_0)^{1/2}$ and $\alpha_0 (Re_0)^{7/5}$ cannot be selected which give absolute demarcation between type S and type C spin decay. We thus pick values which do the best job of separating the data, and select $\alpha_0 (Re_0)^{1/2} = 4.5 \times 10^2$ or $\alpha_0 (Re_0)^{7/5} = 9.2 \times 10^8$; these curves are plotted in Fig. 10. According to our assumptions type S records are obtained for parameter values less than critical and type C for values greater than critical.

The data are plotted in Fig. 10. A flag on a data point indicates that there was an uncertainty about either the spin record type or α_0. To the left of each curve only type S points are found; to the right of each curve all the type C points are found. These results comply with the theory. If the flagged points are weighted equally with the others, the correlation is

only moderately successful. With omission of the flagged points the correlation is completely successful. Perhaps there is a broad band of α_0, Re_0 values above critical where either type S or type C can occur; a definite conclusion cannot be reached because of the uncertainty in the flagged points. Possibly other parameters, not measured in these tests, e.g., the initial yawing rate, will have to be included in the analysis to develop more successful correlating parameters.

Spin Decay from Conjectured Instability

The hypothesized nonlinear instability during spin-up must be supplemented by a flow model and a method of estimating torque. References 6 and 7 describe these and the method for computing spin decay. The essentials are repeated here. An estimate for the torque T in Eq. (1) was made by modifying a flow model described by Batchelor in the Appendix to Ref. 9:

$$T(t) \approx K(2c)a^4 \rho p^2 Re_0^{-1/2} [a/D(t)]^{1/4} \tag{16}$$

where $D(t)$ is the distance of the Wedemeyer shear layer from the cylinder sidewall (see first paragraph of third section) and K is a constant not provided by the model. For early times, $D(t)$ is approximated by[1]

$$D(t) \approx 0.433\ (a^2/c) Re_0^{-1/2} pt \quad \text{(laminar Ekman layer)} \tag{17}$$

$$D(t) \approx 0.035 (a^2/c) Re_0^{-1/5} pt \quad \text{(turbulent Ekman layer)} \tag{18}$$

An additional assumption is needed to obtain K since there are no torque measurements for our configuration. We assume it can be estimated from rotating cylinder data. We used the data of Wendt in Fig. 10 of Ref. 9 since it extends to the large Re_0 required. The gap width is taken to be $D(t)$, with $t=0.5$ s. The parameters of round 5 were used to obtain the torque. Substituting these parameters and this torque into Eq. (16) gives $K=1.44$. To estimate spin decay we integrate Eq. (1), including M. Since rounds 5 and 6 have similar launch conditions, we take an average, $p_0=102.5$ rev/s, in the calculation.

Equation (1) is integrated in two stages: 1) for $0 \le t \le t_c$ with T given by Eq. (16); and 2) for $t > t_c$ with $T=0$, i.e., aerodynamic damping only. The time t_c is the time at which p_c, the solid-body spin rate, is reached; p_c can be estimated in the following manner. The integration of Eqs. (1) and (2), based on the approximations $M(t)=0$ (at early times), $L(t=0)=0$, and $L(t=t_c) \approx \pi \rho a^4\, cp_c \beta(2-\beta)$, lead to

$$p_c \approx I_z p_0 / [I_z + \pi \rho c a^4 \beta (2-\beta)]$$

where β is the ratio of liquid volume to total volume. It is also found that $p_0 - p \sim t^{3/4}$ at early times.

The numerical results based on our conjecture are compared with yawsonde measurements in Fig. 9 for rounds 5 and 6. The agreement for round 6 is surprisingly good, considering the tenuous nature of our theory. The conservative conclusion from this calculation is that our conjecture and assumptions are not contradicted by the firing test data. It is realized that other mechanisms, not considered here, may play a role in producing type C spin decay. Note that we have not included the effect of the nutational motion of the projectile on the fluid; we do not know how to account for this at present.

Conclusions

The authors have developed a numerical method (method I) to predict the spin-decay history of a spin-stabilized liquid-filled projectile. This model takes into account both aerodynamic spin damping and the effect of liquid spin-up in the gun barrel. Wedemeyer's approximate model of spin-up flow in a liquid-filled cylinder forms the basis for this work. Comparison of calculations for 155-mm liquid-filled projectiles with yawsonde measurements have shown favorable agreement for cases of very small yaw.

For some projectiles launched with $\alpha_0 \ge 4$ deg the spin records exhibit behavior which cannot be described by the aboye model; namely, a rapid initial spin decay, followed by a "corner" or discontinuity in slope. A criterion, depending only on α_0 and Re_0, for determining the existence or nonexistence of a corner-type record was derived on the basis of a conjectured nonlinear instability in the spin-up flow. In addition, a flow model incorporating toroidal vortices was employed to predict such anomalous spin records. The authors are aware, however, that a final conclusive explanation has not yet been demonstrated. They feel, nevertheless, that the methods described in this paper will accurately predict the spin history of liquid-filled projectiles launched at very small yaw.

Acknowledgments

The authors thank J. M. Bartos for developing computer programs used for the numerical calculations with method II. The authors are grateful to W. P. D'Amico Jr. and A. Mark for supplying the yawsonde data and their interpretation, and also S. Davis, of Johns Hopkins University, for helpful discussions concerning possible instabilities associated with the spin-decay records having corners.

References

[1] Wedemeyer, E. H., "The Unsteady Flow Within a Spinning Cylinder," *Journal of Fluid Mechanics*, Vol. 20, Pt. 3, 1964, pp. 383-399; also see BRL Rept. 1252, Aberdeen Proving Ground, Md., AD431846, Oct. 1963.

[2] Mark, A. and Mermagen, W. H., "Measurement of Spin Decay and Instability of Liquid-Filled Projectiles Via Telemetry," BRL Memorandum Rept. 2333, Aberdeen Proving Ground, Md., AD771919, Oct. 1973; also see Mark, A., "Transient Eigenfrequencies in Liquid-Filled Cylinders," *AIAA Journal*, Vol. 13, Feb. 1975, pp. 217-219.

[3] Sedney, R. and Gerber, N., "Viscous Effects in the Wedemeyer Model of Spin-Up From Rest," BRL Rept. (in preparation).

[4] Kitchens, C. W., Jr. and Gerber, N., "Prediction of Spin Decay of Liquid-Filled Projectiles," BRL Rept. 1996, Aberdeen Proving Ground, Md., AD A043275, July 1977.

[5] Kitchens, C. W., Jr., "Navier-Stokes Solutions for Spin-Up From Rest in a Cylindrical Container," BRL Rept., (in preparation).

[6] Kitchens, C. W., Jr., Gerber, N., and Sedney, R., "Spin Decay Prediction for Gun-Launched Liquid-Filled Projectiles," AIAA Paper 77-1158, AIAA Flight Mechanics Conference, Hollywood, Fla., Aug. 1977.

[7] Kitchens, C. W., Jr. and Sedney, R., "Conjecture for Anomalous Spin Decay of the 155mm Binary Shell (XM687)," BRL Rept. 2026, Aberdeen Proving Ground, Md., AD A050311, Oct. 1977.

[8] Kitchens, C. W., Jr., Gerber, N., and Sedney, R., "Oscillations of a Liquid in a Rotating Cylinder: Part II. Spin-Up," BRL Rept., (in preparation).

[9] Donnelly, R. J. and Simon, N. J., "An Empirical Torque Relation for Supercritical Flow Between Rotating Cylinders," *Journal of Fluid Mechanics*, Vol. 7, Part 3, 1960, pp. 401-418.